Title: CXCR3A promotes the secretion of the anti-fibrotic decoy receptor sIL-13Rα2 by pulmonary fibroblasts

Authors: Julie C. Worrell[1], Sinead M Walsh[1, 2], Aurélie Fabre[1, 2, 3], Rosemary Kane[1], Boris Hinz[4], Michael P. Keane[1, 2]

Running Title: CXCR3A regulates fibroblast IL-13Rα2

Affiliations:

[1]St. Vincent's University Hospital and School of Medicine, University College Dublin and UCD Conway Institute of Biomolecular and Biomedical Research, Dublin, Ireland.

[2]UCD Conway Institute of Biomolecular and Biomedical Research, University College Dublin, Ireland.

[3]UCD Conway Research Pathology Core Technology, University College Dublin, Ireland.

[4]Laboratory of Tissue Repair and Regeneration, Faculty of Dentistry, University of Toronto, Toronto, Ontario, Canada.

Corresponding Author: Michael P Keane, UCD School of Medicine, C002 Health Sciences Building, Dublin 4, Ireland.

Tel: +353-1-221-4474 fax: +353-1-221-3750

Email: michael.p.keane@ucd.ie

Conflict of interest statement: The authors have declared that no conflict of interest exists.

Abstract

CXCR3A and its IFN-inducible ligands CXCL9 and CXCL10 regulate vascular remodelling and fibroblast motility. IL-13 is a pro-fibrotic cytokine implicated in the pathogenies of inflammatory and fibro-proliferative conditions. Previous work from our lab has shown that CXCR3A is negatively regulated by IL-13 and is necessary for the basal regulation of the IL-13 receptor subunit IL-13Rα2. This study investigates the regulation of fibroblast phenotype, function and downstream IL-13 signalling by CXCR3A *in vitro*. CXCR3A was overexpressed *via* transient transfection. $CXCR3A^{-/-}$ lung fibroblasts were isolated for functional analysis. Additionally, the contribution of CXCR3A to tissue remodelling following acute lung injury was assessed *in vivo* using wild type (WT) and $CXCR3^{-/-}$ mice challenged with IL-13. CXCR3 and IL-13Rα2 displayed a reciprocal relationship following stimulation with either IL-13 or CXCR3 ligands. CXCR3A reduced expression of fibroblast activation makers, soluble collagen production and proliferation. CXCR3A enhanced the basal expression of pERK1/2 while inducing IL-13 mediated down-regulation of NFκB-p65. $CXCR3A^{-/-}$ pulmonary fibroblasts were increasingly proliferative and displayed reduced contractility and α-smooth muscle actin expression. IL-13 challenge regulated expression of the CXCR3 ligands and soluble IL-13Rα2 levels in lungs and broncho-alveolar lavage fluid (BALF) of WT mice, this response was absent in $CXCR3^{-/-}$ mice. Alveolar macrophage accumulation and expression of genes involved in lung remodelling was increased in $CXCR3^{-/-}$ mice. We conclude that CXCR3A is a central anti-fibrotic factor in pulmonary fibroblasts, limiting fibroblast activation and reducing ECM production. Therefore targeting of CXCR3A may be a novel approach to regulate fibroblast activity in lung fibrosis and remodelling.

Keywords: CXCR3A, fibroblast, fibrosis, contractility, collagen

Introduction

Regulated fibrogenesis and fibroblast activation are essential for the normal wound healing response. Fibroblasts are a heterogenous population of multifunctional extracellular matrix (ECM) protein secreting cells, capable of undergoing activation into myofibroblasts (25). This contractile phenotype is defined by expression of contractile proteins and alpha-smooth muscle actin (α-SMA) and is essential for tissue repair and remodelling in the lung (24, 56). Fibroblastic cells are also important sources of growth factors, cytokines and chemokines that directly modulate the immune response occurring during physiological tissue repair (11, 53, 57). The persistence of aberrantly activated fibroblasts regulates the switch from acute resolving to chronic persistent inflammation (11).

Classical CXC chemokine receptor 3 (CXCR3) binds pro-inflammatory non-ELR-motif (glutamate-leucine-arginine motif) chemokines CXCL9, CXCL10 and CXCL11. In humans there are three splice variants of the receptor (CXCR3A, CXCR3B and CXCR3alt), however due to the presence of an in-frame stop codon CXCR3B cannot be functionally translated in mice (13). Mice that lack CXCR3A exhibit more progressive fibrosis and have increased mortality in response to bleomycin insult (28). Administration of ligands CXCL10 and CXCL11 have been shown to ameliorate fibrosis, prevent the recruitment of fibroblasts, and decrease angiogenesis in the lung promoting IFNγ production (12, 27, 30). CXCR3 is expressed by a variety of cell types including epithelial cells, endothelial cells, T-lymphocytes and fibroblasts (35, 37, 48, 51). CXCR3A signalling is important for dermal maturation and matrix remodelling (61, 62). Additionally, CXCR3 ligand-receptor signalling regulates a variety of cell-type specific responses regulating angiogenesis (2), angiostasis (48), tissue remodelling (9) and repair (63). Our group

and others have shown that CXCR3A is expressed by pulmonary fibroblasts (5, 52) and plays a role in the regulation of the interleukin-13 receptor α2 subunit (IL-13Rα2) by pulmonary fibroblasts *in vitro* (5).

Interleukin-13 (IL-13) is a T-Helper Type-2- cytokine that has been implicated in the pathogenesis of fibro-proliferative disorders and potentiates experimentally induced lung injury in numerous experimental settings (6, 8, 31, 32, 64). In human disease, IL-13 drives tissue remodelling responses in asthma (33) and is elevated in chronic fibrotic conditions such as systemic sclerosis (22, 45) and idiopathic pulmonary fibrosis (21, 43, 47). IL-13 binds to receptor chains IL-13Rα1 and IL13Rα2. Generally considered to be a decoy receptor for IL-13 and devoid of signalling activity due to a short cytoplasmic tail (65), IL-13Rα2 binds IL-13 at much higher affinity and specificity than IL-13Rα1 (39). Mice lacking the IL-13Rα2 decoy receptor have enhanced IL-13 activity (59) and research from our group has shown that adenoviral over-expression of IL-13Rα2 limits fibrosis in response to bleomycin induced lung injury (38).

Here, we discover a reciprocal relationship between CXCR3A and IL-13Rα2 following stimulation with CXCR3 ligands. Expression of the CXCR3A splice variant was negatively regulated by IL-13 treatment and dramatically reduced in the bleomycin model of pulmonary fibrosis. Overexpression of CXCR3A *in vitro* in NIH3T3 fibroblasts reduced the pro-fibrogenic activity of these cells, suppressed downstream IL-13 signalling (STAT6, ERK1/2 and NFκBp65) and reduced the secretion of matricellular proteins. CXCR3A$^{-/-}$ fibroblasts secreted more ECM but had reduced contractile capabilities *in vitro.* Following IL-13 challenge, CXCR3A$^{-/-}$ mice displayed dysregulated lung remodelling *in vivo* and increased inflammatory infiltrate (alveolar macrophages). IL-13 induced regulation of the CXCR3 ligands and soluble

IL-13Rα2 was blunted in BALF and lungs of CXCR3A$^{-/-}$ mice compared to wildtype animals. We identify a novel role for CXCR3A in the regulation of fibroblast contractility and secretion of sIL-13Rα2. These findings identify CXCR3A as a potential target in the generation of future anti-fibrotic therapies that modulate fibroblast function.

Results

Data supplements can be found here:

https://doi.org/10.6084/m9.figshare.11902887

CXCL10 regulates the IL-13Rα2 receptor in a CXCR3A dependent manner and affects fibroblast proliferation

Previous work from our lab has identified a role for CXCR3A in basal regulation of the anti-fibrotic decoy receptor IL-13Rα2. To decipher the mechanism of how CXCR3 ligands CXCL9 and CXCL10 exert regulatory effects on this receptor, we now used NIH3T3 fibroblasts *in vitro*. Treatment with CXCR3 ligand CXCL10 resulted in significantly downregulated expression of the CXCR3 receptor (Figure 1A) while upregulating the expression of *Il13rα2* mRNA and IL-13Rα2 protein at 24 h (Figure 1B and 1C). To test which function this exerts on fibroblasts we examined the effect of the ligands on fibroblast proliferation. CXCL10 treatment significantly induced proliferation of NIH3T3 fibroblasts (Figure 1D). CXCL10 has been shown to act independently of CXCR3 (13). To investigate if the regulation of IL-13Rα2 by CXCL10 was dependent on CXCR3A fibroblasts were treated with a CXCR3 antagonist (18) prior to ligand stimulation. In the presence of the antagonist CXCL10 failed to upregulate *Il13rα2* gene expression (Figure 1E). There was no change in cellular viability, determined by the Alamar blue assay (Figure 1F), however fibroblasts treated with the CXCR3 antagonist proliferated significantly less than vehicle controls (Figure 1G). Overall, these data suggest that the CXCR3 ligand CXCL10 regulates expression of IL-13Rα2 and that this regulation by CXCL10 is dependent on the CXCR3A receptor.

CXCR3A reduces fibroblast activation, soluble collagen production and proliferative capacity

We investigated the functional effect of CXCR3A over-expression in fibroblasts. The cellular localisation of CXCR3A (yellow) was visualised by immunofluorescence 24 h post transfection in NIH3T3 fibroblasts transfected with either empty vector control or CXCR3A plasmid, antibody specificity was verified with appropriate isotype control (Figure 2A). The number of CXCR3A positive cells per field of view was higher in CXCR3A transfected fibroblasts compared to empty vector controls. *Cxcr3A* gene expression assessed by qRT-PCR (Figure 2B), cellular viability by Alamar blue (Figure 2C) and CXCR3A protein assessed by western blotting (Figure 2D). CXCR3A gene and protein were significantly increased in transfected fibroblasts compared to empty vector controls. No differences were detected in cellular viability. CXCR3A over-expression altered fibroblast gene expression and functional capabilities. Significant decreases in gene expression of fibroblast activation markers *Acta2*, *Col1a1*, *Vim* and *Fsp1* (Figure 3A-D) were detected in CXCR3A transfected fibroblasts. Additionally, gene expression of the anti-fibrotic receptor *Il13rα2* was significantly elevated (Figure 3E) while fibroblast proliferation was reduced (Figure 3F). Secreted levels of key components of the ECM; soluble collagen and active TGFβ1 (Figure 3G-H) were observed in addition to altered chemokine secretion (Figure 3I-J). However, IFN-γ levels below the limit of detection. These data show that CXCR3A functions as a regulator of fibroblast phenotype by modulating fibroblast activation and by limiting functional capabilities that contribute to tissue fibrosis.

CXCR3A regulates downstream IL-13 signaling and secretion of matricellular proteins

Next, we investigated the effect of CXCR3A over-expression on fibroblast signaling following stimulation with IL-13. STAT6 is a major downstream mediator of IL-13 signalling (49). A time-course of IL-13 stimulation was performed on NIH3T3 fibroblasts transfected with CXCR3A for 24 h to examine, the phosphorylation of downstream signaling molecules STAT6, MAPK pathway ERK1/2 (p44 and p42) and canonical NFκB family member NFκB-p65 (RelA). In CXCR3A overexpressing fibroblasts phosphorylation of all proteins was delayed compared to empty vector controls in a time dependent manner (Figure 4A). STAT6 phosphorylation was delayed in response to IL-13 stimulation in CXCR3A transfected fibroblasts by 15 min compared to empty vector controls. CXCR3A overexpression markedly upregulated pERK1/2 at a basal level with no changes in pERK1/2 observed in response to IL-13 stimulation. In contrast, IL-13 stimulated empty vector controls exhibited peak levels of pERK1/2 after 15-30 min. Interestingly, baseline levels of pNFκB-p65 were reduced in fibroblasts transfected with CXCR3A and stimulation with IL-13 resulted in a dramatic reduction of total NFκB-p65 after 15 min. Thus, CXCR3A overexpression in fibroblasts regulates pERK1/2 and NFκB-p65 at a basal level, promoting activation of the ERK1/2 pathway and downregulation of NFκB-p65. These results may indicate that in the presence of CXCR3A ERK1/2 competes with NFκB signaling.

We have previously shown both membrane-bound IL-13Rα2 (mIL-13Rα2) and the soluble version (sIL-13Rα2) are inhibitory receptors for IL-13 (37). Protein levels of membrane bound (mIL-13Rα2) and soluble (sIL-13Ra2) were measured in NIH3T3 fibroblasts 24 h post CXCR3A-transfection with and without IL-13 stimulation for 24

h. sIL-13Rα2. Alterations in protein levels of mIL-13Rα2 (upper band) and sIL-13Rα2 (lower band) were detected (Figure 4B). sIL-13Rα2 levels was elevated in CXCR3A overexpressing fibroblasts which was more pronounced upon IL-13 stimulation (Figure 4B). Since these results suggest that CXCR3A may also be important for the decoy function of IL-13Rα2, soluble levels of IL-13Rα2 in cell supernatants were examined by ELISA. The levels of secreted sIL-13Rα2 were significantly elevated in IL-13 treated CXCR3A overexpressing fibroblasts compared to empty vector controls (Figure 4C). Periostin is an ECM protein with a matricellular function and its expression is induced by IL-13 (40). Secretion of periostin was significantly reduced in CXCR3A transfected fibroblasts following IL-13 stimulation (Figure 4D). Collectively, these results show that CXCR3A alters signaling downstream of IL-13 and exerts a regulatory function on the availability of the sIL-13Rα2, impacting secretion of matricellular proteins.

CXCR3A-negative fibroblasts are less contractile and produce more ECM

Given the ability of CXCR3A to potentiate anti-fibrotic effects at baseline and in the presence of IL-13 we next performed functional assays with fibroblasts isolated from global CXCR3A$^{-/-}$ mice. We used elastic 'wrinkling' silicone substrates to measure cell contractility following stimulation with IL-13 (Figure 5) (23). Wrinkling force of WT and CXCR3A$^{-/-}$ fibroblasts was quantified by thresholding and binarizing images for phase-bright wrinkle signals (Figure 5A-C). WT fibroblasts produced larger substrate wrinkles, compared with smaller and lower abundance wrinkles produced by CXCR3A$^{-/-}$ fibroblasts. Without IL-13 stimulation, CXCR3A$^{-/-}$ fibroblasts displayed increased proliferative capacity (Figure 5D) and produced more soluble collagen

(Figure 5E). At the protein level Col1A1 protein was elevated accompanied by increased expression of intermediate filament protein vimentin, however α-SMA expression was decreased in CXCR3A$^{-/-}$ fibroblasts (Figure 5F). α-SMA is important for contractility of fibroblasts and is a key marker of myofibroblast activation. The results of the functional assays indicate CXCR3A$^{-/-}$ fibroblasts are unlikely to be contractile αSMA+ myofibroblasts and are more likely to be static matrix producing fibroblasts.

IL-13 regulates chemokine expression and induces alveolar macrophage accumulation *in vivo*

In order to evaluate the biological significance of our *in vitro* data, WT and CXCRA$^{-/-}$ mice were intranasally instilled with IL-13 for 24 h. To assess inflammatory response and measures of lung remodelling differential cell counts from the bronchial alveolar lavage fluid), cytokine/chemokine concentrations in BALF and whole lungs were examined. The total number of cells in BALF was significantly increased in IL-13-challenged CXCR3A$^{-/-}$ mice when compared to vehicle control WT mice (Figure 6A). The total protein content in BALF was measured (broad measure of vascular permeability) and no significant differences were observed (Supplemental Figure 1A). Assessment of chemokine levels in BALF revealed a significant induction of CXCL10 levels in WT lungs treated with IL-13 compared to vehicle controls (Figure 6B). Lung macrophages are an important source of CXCL10 following injury (55). No significant differences were observed in CXCL9 levels in BALF, while soluble IL-13Rα2 was elevated in 4/5 samples following IL-13 stimulation (Supplemental Figure 1B-C). Diffquik staining (MGG) was used to identify cell populations in the BALF. All cells were mononuclear (indicated by black arrows) with large cytoplasmic space, suggesting they are macrophages that were recruited to the lung

airspace following IL-13 induced injury (Figure 6C). Expression of CXCR3 ligands CXCL9 and CXCL10 was reduced in WT mice following IL-13 treatment (Figure 6D-E), IL-13 treatment also downregulated CXCL10 expression in CXCR3A$^{-/-}$ mice. Soluble IL-13Rα2 levels were markedly reduced in WT lungs treated with IL-13 but this response was blunted in CXCR3A$^{-/-}$mice with levels remaining close to vehicle controls (Figure 6F). *Ccl17*, *Ccl22* and *Il13ra2* gene expression levels were quantified as measures of lung remodelling, *Il13ra2* mRNA also served as measure of IL-13 response. *Ccl17* was significantly elevated in CXCR3A$^{-/-}$ mice challenged with IL-13 compared to IL-13 challenged WT mice (Supplemental Figure 1D), no differences were observed in *Ccl22* levels (Supplemental Figure 1E). No significant differences were observed in the induction of IL-13Rα2 between WT and CXCR3A$^{-/-}$ treated with IL-13 at the gene level. It should be noted that the qPCR primer used does not discriminate between transcripts for the membrane bound and the soluble form of the receptor (Supplemental Figure 1F). CXCR3A$^{-/-}$ mice appear to have an enhanced lung remodelling response following IL-13 stimulation caused by increased accumulation of alveolar macrophages and dysregulated expression of chemokines in the lung. These *in vivo* findings suggest that in the injured CXCR3A$^{-/-}$ lung communication between macrophages and stromal cells is altered, potentially limiting effective tissue repair.

CXCR3A is negatively regulated by IL-13 stimulation *in vitro* and during peak fibrotic phase of bleomycin induced lung injury

We next investigated the effect of IL-13 stimulation on CXCR3A expression. IL-13 stimulation resulted in significantly downregulated *Cxcr3A* gene (Figure 7A) and protein expression 7B. Reduced sIL-13Rα2 levels were detected following IL-13

stimulation (Figure7C). Taken together, these data highlight IL-13 negatively regulates expression of anti-fibrotic receptors CXCR3A and sIL-13Rα2 in fibroblasts, *in vitro.* As IL-13 is also a major driver of tissue remodelling and fibrosis, we examined *Cxcr3A* gene expression in both peak inflammatory phase (day 5) and fibrotic phase (day 21) of the bleomycin model of lung injury. CXCR3 expression was significantly downregulated in lungs at day 21 post bleomycin instillation compared to vehicle controls (Figure 7D); no change was observed at day 5. Expression of CXCR3A is limited in the context of acute injury induced by *in vitro* IL-13 stimulation and in chronic lung fibrosis.

Discussion

This study provides multiple lines of evidence that CXCR3A regulates fibroblast function and phenotype *in vitro*, constraining fibroblast proliferation, matrix secretion and release of pro-fibrotic soluble mediators. We have highlighted a novel role for CXCR3A in regulation of fibroblast contractility, in the absence of CXCR3A fibroblasts have reduced contractile capacity and α-SMA levels. Additionally, CXCR3A is an upstream regulator of both ERK1/2 and NFκB-p65 signalling, both at a basal level and in the presence of IL-13. Furthermore, CXCR3 promotes the secretion anti-fibrotic decoy receptor sIL-13Rα2. This is a novel role for the receptor independent of its previously recognised role as a regulator cellular proliferation and chemotaxis. Our i*n vivo* findings demonstrate that IL-13 regulates CXCR3 ligand expression levels in the lungs and BALF of WT mice. $CXCR3A^{-/-}$ mice have increased accumulation of alveolar macrophages and a more pronounced lung remodelling response following acute lung injury. These findings make this investigation directly relevant to lung conditions involving lung remodelling and/or tissue fibrosis.

This study adds to our previous findings that CXCR3 is necessary for the basal regulation of IL-13Rα2 on cultured pulmonary fibroblasts (5). We focused on CXCL9 and CXCL10 because C57BL/6 mice do not express CXCL11 due to a frameshift within the coding sequence that leads to a premature stop codon (14). Here, we show the CXCR3 ligand CXCL10 is responsible for the up-regulation of IL-13Rα2 by fibroblasts, by acting directly through its own receptor. Functional CXCR3 receptor expression has been detected on other stromal cell subtypes e.g. hepatic stellate cells (10) intestinal myofibroblasts (34) and fibroblast-like synovicytes (36) where engagement by CXCL10 stimulated proliferation and/or chemotaxis. CXCL10 is

downregulated in pulmonary fibrosis (30), we observed reduced CXCR3A levels at day 21 post bleomycin instillation but not during the inflammatory phase. Peak expression of IL-13 receptor subunits occurs at day 21 and 28 following bleomycin instillation (26). Under normal homeostatic conditions CXCR3A and its ligands downregulate Th_2 responses while promoting Th_1 cell migration, our data suggest CXCR3A also regulates fibroblast accumulation following lung injury to sites of tissue injury. This may be regulated *via* the CXCR3 receptor itself or by modulation of cellular crosstalk between fibroblasts and recruited immune cells following lung injury.

Previous i*n vivo* studies investigating CXCR3 in pulmonary fibrosis by Jiang *et al.,* have largely neglected and/or underestimated the fibroblast specific expression of the receptor. Instead focusing the Th1 response and the impact of CXCR3 expression by immune cells (CD8 T cells and NK cells) on fibroproliferation(28) or suggesting the that the actions of CXCL10 were largely independent of CXCR3 (27). This is the first investigation, to our knowledge, involving the over-expression of CXCR3A in fibroblasts where direct effects on fibroblast phenotype have been examined. Previous research has focused ligand-receptor interactions and mechanisms of CXCR3 receptor internalisation (41, 42), while our study shows a dramatic reduction in fibroblast activation and production of soluble mediators

Yates *et al*., have demonstrated CXCR3A receptor expression by fibroblasts regulates dermal maturation and when CXCR3A is absent total skin collagen content is reduced, accompanied by immature and disorganised fibrillar collagen (63). The apparent disparity in results between investigations could be due to several reasons including differing methodologies and anatomical locations. We demonstrated reduced collagen secretion in the presence of CXCR3A, while in the absence of

CXCR3A soluble collagen content was increased. The Sircol assay detects only the soluble forms of collagen types I-IV. It does not quantify insoluble collagen content and does not discriminate between different collagen isoforms or assess maturity of the collagen produced. Additionally, fibroblasts isolated from different tissues display similar morphology but can exhibit different functional properties, a concept termed 'positional memory' (16). Anatomical considerations such a tensile strength and fibrillar collagen organization will also differ between skin and lung.

Elevated secretion of CXCL9 was accompanied by a decrease in active TGFβ1 secretion, CXCL9 prevents epithelial to mesenchymal transition of lung epithelial cells by abrogating TGFβ1 induced SMAD2/3 phosphorylation *in vitro* (44). Interestingly, in addition to regulating canonical downstream IL-13 signalling e.g. STAT6 and MAPK-ERK pathways, in the presence of the CXCR3A plasmid, IL-13 stimulation induced NFκB-p65 degradation at 15 mins. Activation of ERK1/2 and inhibition of NFκB may be due to direct competition between ERK1/2 and NFκB-p65. Alternately, this could be mediated *via* up regulation of IκBα which usually serves to constrain NFκB activation, though we cannot exclude the involvement of multiple independent pathways. In dermal fibroblasts expression of NFκB-p65 has been shown to determine extent of collagen synthesis, both in healthy and systemic sclerosis patient samples (7) and in our study CXCR3A expression was also associated with Col1a1 regulation. $CXCR3A^{-/-}$ fibroblasts displayed increased levels of Col1a1 and vimentin protein expression, a recent study by Wohlfahrt *et al.,* has used expression levels of these proteins to distinguish between inflammatory and fibrotic fibroblasts (58). Though $CXCR3A^{-/-}$ fibroblasts appear to have reduced contractile ability, their phenotype is consistent with a matrix-producing pro-fibrotic phenotype.

IL-13Rα2 can act as a decoy receptor capable of binding ligand and thus preventing productive signaling through Rα1. The soluble form of the receptor (ΔEx10 variant of the protein) lacks the transmembrane region of the full-length protein. We suggest that CXCR3A expression may be important in the decoy function of IL-13Rα2. Secretion of soluble IL-13Rα2 protein is more pronounced in the presence of both CXCR3A and IL-13 *in vitro*. Our *in vivo* findings suggest that IL-13 is 'mopped up' by the soluble receptor in lungs of WT mice, but in CXCR3A$^{-/-}$mice this decoy function is potentially absent. However, this was not assessed directly in this investigation. It should be noted that for gene expression analysis the IL-13Rα2 primer used does not detect the ΔEx10 splice variant. There have been reports of signalling activity by IL-13Rα2 in macrophages and in a murine model of pulmonary hypertension (17, 19). However, we propose that IL-13Rα2 serves to limit IL-13 activity/bio-availability, consistent with investigations in lung fibroblasts by Chandriani and colleagues (15).

We also highlight IL-13 mediated regulation of CXCL9 and CXCL10 in the lung *in vivo.* IL-13 up-regulates of CXCL10 protein in BALF, conversely, levels of CXCR3 ligands were decreased in lung homogenates. We identified alveolar macrophages as the predominant population of cells in the BALF, while lung homogenates contain a variety of lymphoid, myeloid, epithelial and stromal cells. IL-13 mediated regulation of the CXCR3 ligands may be dependent on cell type. CXCL10 is highly expressed by M1 type macrophages, these macrophages contribute to inflammation. IL-13 is a key regulator of macrophage polarisation into and M2 or alternatively activated state (60) these macrophages usually facilitate resolution through secretion of ECM degrading enzymes. Macrophages that lack CXCR3A have a more M2 phenotype (46) and in a model of breast cancer this contributed to increased accumulation of tumor

promoting myeloid derived immune cell populations. In the context of our study, these results suggest dysregulated fibroblast-macrophage cross talk, that may promote the accumulation and retention of fibroblasts within the CXCR3A$^{-/-}$ lung. *Ccl17* gene expression was elevated in CXCR3A$^{-/-}$ mice following IL-13 challenge. CCL17 is chemotactic for fibroblasts and accelerates wound healing by enhancing fibroblast migration (29). This accumulation/retention could impair the ability of both macrophages and fibroblasts to successfully co-ordinate tissue repair, becoming a self-sustaining aberrant process.

The contrasting findings involving cellular proliferation in our study warrant further discussion. Treatment of NIH3T3 fibroblasts with either a CXCR3 antagonist or ectopic overexpression of CXCR3A resulted in a significant decrease in cell proliferation, with no alteration in cellular viability. Previous findings in stromal cells (epithelial cells and endothelial cells) determined that CXCR3 is expressed at the cell surface during a portion of the cell cycle (1, 50). The population of cells expressing CXCR3 on their surface were more likely to be in the late S to G2/M phase of the cell cycle(50). It is possible that both approaches (antagonism and overexpression) result in CXCR3 receptor internalisation or alteration of the cell cycle. We have used a colorimetric BrdU assay as a 'global readout' of DNA synthesis/proliferation. Approaches to quantify BrdU staining combined with CXCR3 surface expression using immunofluorescence would facilitate additional profiling of the BrdU+ cells. CXCR3A-/- fibroblasts were more proliferative than wild type cells, these cells may exist in a constitutively active and/or proliferative state to compensate for the complete absence of CXCR3.

In order to further dissect the cell specific contributions of CXCR3A to stromal-immune cell cross-talk, conditional and/or inducible cell specific knockouts

are preferable to global knockout mice. Such models help to further elucidate compensatory mechanisms that may exist between different cell types, we acknowledge that the use of a CXCR3A global knockout is a limitation of our study. It is difficult to dissect the role of the CXCR3 ligands *in vivo*, these ligands exert context dependent regulation on their receptor in addition to having redundant, collaborative and antagonistic functions. CXCL9 and CXCL10 are highly promiscuous ligands with numerous potential binding partners including multiple chemokine receptors, atypical chemokine receptors and glycosaminoglycans. CXCR3 reporter mice (REX3) have previously been employed in studies by Groom and colleagues to allow reporting of expression of CXCR3 ligands by lymphocytes *in vivo* (20) and could provide valuable insight if the same approach was employed for stromal cells.

This study demonstrates that CXCR3A is a key regulator of fibroblast phenotype i*n vitro* and regulates extracellular matrix production and cellular contractility in pulmonary fibroblasts. IL-13 stimulation exerts discrete effects on CXCR3 ligand expression in the lung *in vivo* that appears to be dependent on cell type e.g. immune and/or stromal cells. This has far reaching implications for CXCR3A as a regulator of cellular communication and as a key driver of decisions within the tissue following lung injury. CXCR3A may act as a 'phenotypic switch' preventing prolonged 'active' or aberrant remodelling processes and promoting tissue repair and resolution**.** Strategies to target or harness the potential of CXCR3A may help to identify novel treatments for a variety of fibrotic conditions.

Materials and Methods

Animals

CXCR3$^{-/-}$ (B6.129P2-Cxcr3tm1Dgen/J, Jackson laboratories) and wild type female C57Bl6/J mice were obtained from Charles River. Animals were maintained under specific pathogen-free conditions in line with Irish and European Union regulations. Experiments were approved by local ethical review and were carried out under the authority of Ireland's project license. 10µg of recombinant murine IL-13 (Biolegend) or PBS was administered intranasally, in a volume of 50µl, for 24 h. Pulmonary fibrosis was induced as previously described (54). Briefly, 8- to 10-wk C57BL/6 mice were anesthetized with ketamine/xylazine and instilled intratracheally with 1 U/kg bleomycin. Animals were euthanized *via* intraperitoneal overdose of sodium pentobarbital, 250 mg/kg.

Cells and Reagents

NIH-3T3 fibroblasts were obtained from European Collection of Cell Cultures (ECACC) and cultured in Dulbecco's Modified Eagle Medium (Gibco/Invitrogen, Ireland) supplemented with 10% heat inactivated FBS, (Sigma Aldrich, Ireland), 5mM L-glutamine (Gibco/Invitrogen) penicillin (100U/ml), and streptomycin (100µg/ml) (Gibco/Invitrogen) at 37° Celsius in humidified 5% CO2. Primary lung fibroblasts were isolated from CXCR3$^{-/-}$mice (B6.129P2-Cxcr3tm1Dgen/J, Jackson laboratories) or wild type C57BL/6 mice (Charles River, UK.) as previously described (3). Primary fibroblasts were used between passages 2-8 for all experiments and cultured in standard media conditions, as above. To prepare samples for analysis, cells were serum starved for 18h then incubated in medium containing vehicle alone or supplemented with IL-13 (Biolegend) CXCL9, CXCL10 (Biolegend) at the time

periods indicated. To investigate CXCR3 dependent signalling cells were pre-treated with 500nM of CXCR3 antagonist 500586 (Calbiochem) for one hour before stimulation with cytokines/chemokines.

Transfection

NIH-3T3 fibroblasts were seeded at 1 x 10^5 cells per well and transfected with a complex formed using TRANSIT 2020 reagent (Mirus, Madison, WI) in Optimem (Gibco, life technologies, Carlsbad, CA) and 1μg of pCMV6-CXCR3-tGFP or empty vector control (Origene, Cambridge, UK). Cells were then serum starved overnight prior to treatment with cytokines.

Sircol Assay

The Sircol Soluble Collagen Assay (Biocolor, Carrickfergus, UK) protocol was performed as per manufacturers' instructions.

Proliferation Assay

Cellular proliferation was measured using the BrdU assay (Roche, Basel, Switzerland) as per the manufacturers' instructions.

ELISA

ELISA experiments performed on cell supernatants, mouse lung homogenates and BAL fluid to detect active-TGFβ1, soluble IL-13Rα2, CXCL9 and CXCL10 (R&D Systems, Wiesbaden, Germany), were performed as per the manufacturers' instructions

Alamar blue assay

Briefly, Resazurin salt (Sigma) stock was dissolved in PBS and sodium hydroxide and used at final concentration 44μM in complete culture medium. After the desired incubation time with drug/treatment, the medium was removed and replaced with fresh medium containing resazurin salt. Cells were incubated for 2 hours with the diluted resazurin and kept out of direct light at 37ºC. The supernatant from each well was removed to a 96 well plate in duplicate and measured at 535nm/595nm in a Spectra Max (Grodig, Austria) plate reader.

Contractility Assay

Cell contractility was assessed using deformable silicone substrates as previously described (11). In brief, polydimethylsiloxane substrates with a Young's modulus of 5 kPa were coated with 10 μg/ml fibronectin for sparse cell cultures. Wrinkle formation on substrates, indicating cell contraction, was observed after 24 h in culture with IL-13. Live phase contrast images were acquired with an inverted microscope (Olympus 200 phase contrast microscope, 10x objective) and analyzed using ImageJ customized macros (U.S. National Institutes of Health, NIH, Bethesda, Maryland, USA, http://imagej.nih.gov/ij/, 1997-2013) by thresholding for phase-bright wrinkles and analyzing the surface area covered by identified particles in the resulting binary images. Relative contraction was expressed as image area covered by wrinkles normalized to cell numbers (4).

Immunofluorescence

NIH-3T3 fibroblasts were seeded at $1x10^5$ cells per mL on sterile 8 well glass chamber slides (Nunc). NIH-3T3 fibroblasts were fixed in 100% methanol (Sigma)

and blocked by incubation in 5% BSA (Sigma). They were then incubated with an 1:400 anti-CXCR3 antibody labelled with PE (ab95724)or 1:400 appropriate isotype control (ab101026; Abcam, Cambridge, UK). Nuclei were counterstained with DAPI (Invitrogen) and images obtained using a Zeiss Axio Imager M1 microscope.

Western Blotting

NIH-3T3 fibroblast whole cell extracts (WCE) were obtained using RIPA buffer (Sigma Aldrich) and Western blotting carried out as previously described (38). Antibodies used were as follows: 1:250 anti-IL 13Rα2 (AF539;R&D Systems), 1:500 anti-CXCR3 (MAB160;R&D Systems), 1:500 anti-phosphorylated-STAT6 (#9361), 1:1000 anti-total STAT6 (#9262), 1:1000 anti-phospho ERK1/2 (#9101), 1:500 anti-total ERK1/2 (#9102), 1:1000anti-phospho NFκB p65 (#3033), 1:1000 anti-total NFκB p65 (#3034), 1:10000 anti-GAPDH (#2118), 1:1000 anti-vimentin antibody (#3932) (Cell Signaling Technology, UK), 1:500 anti α-SMA (A2547), 1:10000 anti-β-actin (A5316) (Sigma Aldrich), 1;10000anti-Fibronectin (610077;BD Biosciences) and 1:200 anti-Col1a1 (Sc-8784; Santa Cruz Biotechnology) Appropriate secondary HRP-conjugated secondary antibodies were used (Cell Signalling Technology).

Quantitative real-time PCR

Total RNA was isolated using the RNeasy plus kit (Qiagen, Manchester, UK)) according to manufacturer's instructions and500 ng of RNA was reverse transcribed to cDNA as per manufacturer's instructions. Quantitative real-time PCR (qRT-PCR) was performed using TaqMan Universal PCR master mix (Applied Biosystems), template cDNA and TaqMan Gene Expression assays (Il-13rα2 Mm_01324829_m1, Cxcl10 Mm_00445253_m1, Cxcl9 Mm_00434946_m1, Cxcr3 Mm_99999054_m1,

Vim Mm_01333430_s1, Fsp1 Mm_00803374_g1, acta2 Mm_01546133_m1, Col1a1 Mm_00801666_g1) on an ABI Prism 7900HT Sequence Detector (Applied Biosystems). 18S rRNA served as an endogenous control. Relative changes in transcript levels in treated samples compared to controls was expressed using the ΔΔCt method.

Statistics

All experiments were performed independently at least three times. Data were analysed GraphPad Prism version 5.01 for Windows (GraphPad, San Diego, California, USA). Data was tested for normality using the Kolmogorov-Smirnov test with (α=0.05). Data are presented as mean ± SEM and P values were calculated using two-tailed Student's *t*-test for pairwise comparison of variables, one-way ANOVA for multiple comparison of variables, and two-way ANOVA involving two independent variables. A Sidak's multiple comparisons test was used. P values < 0.05 were considered significant.

Author Contributions: J.C.W, R.K and M.P.K conception and design of research; J.C.W and S.M.W performed experiments; J.C.W, S.M.W and B.H. analyzed data; S.M.W, J.C.W, A.F, R.K, B.H and M.P.K interpreted results of experiments; J.C.W prepared figures, J.C.W drafted manuscript; J.C.W, S.M.W, A.F, R.K, B.H and M.P.K edited and revised manuscript, all authors approved the final version of manuscript.

Funding: J.C.W was supported by Molecular Medicine Ireland Clinical and Translational Research Scholars Programme, funded under PRTLI Cycle 5 and

539 ERDF. B. Hinz is supported by Canadian Institutes of Health Research Foundation
540 Grant 375597.

541

542 **Acknowledgements**

543 We acknowledge the excellent technical assistance provided by the Conway Institute
544 Core Facility, including Catherine Moss, Dimitri Scholtz, and Janet McCormack, and
545 the excellent technical assistance of Stellar Boo (University of Toronto) in preparing
546 wrinkling silicone substrates.

References

1. **Aksoy MO, Yang Y, Ji R, Reddy PJ, Shahabuddin S, Litvin J, Rogers TJ, and Kelsen SG**. CXCR3 surface expression in human airway epithelial cells: cell cycle dependence and effect on cell proliferation. *American journal of physiology Lung cellular and molecular physiology* 290: L909-918, 2006.
2. **Angiolillo AL, Sgadari C, Taub DD, Liao F, Farber JM, Maheshwari S, Kleinman HK, Reaman GH, and Tosato G**. Human interferon-inducible protein 10 is a potent inhibitor of angiogenesis in vivo. *The Journal of experimental medicine* 182: 155-162, 1995.
3. **Baglole CJ, Reddy SY, Pollock SJ, Feldon SE, Sime PJ, Smith TJ, and Phipps RP**. Isolation and phenotypic characterization of lung fibroblasts. *Methods in molecular medicine* 117: 115-127, 2005.
4. **Balestrini JL, Chaudhry S, Sarrazy V, Koehler A, and Hinz B**. The mechanical memory of lung myofibroblasts. *Integrative biology : quantitative biosciences from nano to macro* 4: 410-421, 2012.
5. **Barnes JC, Lumsden RV, Worrell J, Counihan IP, O'Beirne SL, Belperio JA, Fabre A, Donnelly SC, Boylan D, Kane R, and Keane MP**. CXCR3 Requirement for the Interleukin-13-Mediated Up-Regulation of Interleukin-13Ralpha2 in Pulmonary Fibroblasts. *American journal of respiratory cell and molecular biology* 53: 217-225, 2015.
6. **Belperio JA, Dy M, Burdick MD, Xue YY, Li K, Elias JA, and Keane MP**. Interaction of IL-13 and C10 in the pathogenesis of bleomycin-induced pulmonary fibrosis. *American journal of respiratory cell and molecular biology* 27: 419-427, 2002.
7. **Bigot N, Beauchef G, Hervieu M, Oddos T, Demoor M, Boumediene K, and Galera P**. NF-kappaB accumulation associated with COL1A1 transactivators defects during chronological aging represses type I collagen expression through a -112/-61-bp region of the COL1A1 promoter in human skin fibroblasts. *The Journal of investigative dermatology* 132: 2360-2367, 2012.
8. **Blease K, Schuh JM, Jakubzick C, Lukacs NW, Kunkel SL, Joshi BH, Puri RK, Kaplan MH, and Hogaboam CM**. Stat6-deficient mice develop airway hyperresponsiveness and peribronchial fibrosis during chronic fungal asthma. *The American journal of pathology* 160: 481-490, 2002.
9. **Bodnar RJ, Rodgers ME, Chen WC, and Wells A**. Pericyte regulation of vascular remodeling through the CXC receptor 3. *Arteriosclerosis, thrombosis, and vascular biology* 33: 2818-2829, 2013.
10. **Bonacchi A, Romagnani P, Romanelli RG, Efsen E, Annunziato F, Lasagni L, Francalanci M, Serio M, Laffi G, Pinzani M, Gentilini P, and Marra F**. Signal transduction by the chemokine receptor CXCR3: activation of Ras/ERK, Src, and phosphatidylinositol 3-kinase/Akt controls cell migration and proliferation in human vascular pericytes. *The Journal of biological chemistry* 276: 9945-9954, 2001.
11. **Buckley CD, Pilling D, Lord JM, Akbar AN, Scheel-Toellner D, and Salmon M**. Fibroblasts regulate the switch from acute resolving to chronic persistent inflammation. *Trends in immunology* 22: 199-204, 2001.
12. **Burdick MD, Murray LA, Keane MP, Xue YY, Zisman DA, Belperio JA, and Strieter RM**. CXCL11 attenuates bleomycin-induced pulmonary fibrosis via inhibition of vascular remodeling. *American journal of respiratory and critical care medicine* 171: 261-268, 2005.

13. **Campanella GS, Colvin RA, and Luster AD**. CXCL10 can inhibit endothelial cell proliferation independently of CXCR3. *PloS one* 5: e12700, 2010.
14. **Carr DJ, Wuest T, and Ash J**. An increase in herpes simplex virus type 1 in the anterior segment of the eye is linked to a deficiency in NK cell infiltration in mice deficient in CXCR3. *Journal of interferon & cytokine research : the official journal of the International Society for Interferon and Cytokine Research* 28: 245-251, 2008.
15. **Chandriani S, DePianto DJ, N'Diaye EN, Abbas AR, Jackman J, Bevers J, 3rd, Ramirez-Carrozzi V, Pappu R, Kauder SE, Toy K, Ha C, Modrusan Z, Wu LC, Collard HR, Wolters PJ, Egen JG, and Arron JR**. Endogenously expressed IL-13Ralpha2 attenuates IL-13-mediated responses but does not activate signaling in human lung fibroblasts. *Journal of immunology (Baltimore, Md : 1950)* 193: 111-119, 2014.
16. **Chang HY, Chi JT, Dudoit S, Bondre C, van de Rijn M, Botstein D, and Brown PO**. Diversity, topographic differentiation, and positional memory in human fibroblasts. *Proceedings of the National Academy of Sciences of the United States of America* 99: 12877-12882, 2002.
17. **Cho WK, Lee CM, Kang MJ, Huang Y, Giordano FJ, Lee PJ, Trow TK, Homer RJ, Sessa WC, Elias JA, and Lee CG**. IL-13 receptor alpha2-arginase 2 pathway mediates IL-13-induced pulmonary hypertension. *American journal of physiology Lung cellular and molecular physiology* 304: L112-124, 2013.
18. **Crosignani S, Missotten M, Cleva C, Dondi R, Ratinaud Y, Humbert Y, Mandal AB, Bombrun A, Power C, Chollet A, and Proudfoot A**. Discovery of a novel series of CXCR3 antagonists. *Bioorganic & medicinal chemistry letters* 20: 3614-3617, 2010.
19. **Fichtner-Feigl S, Strober W, Kawakami K, Puri RK, and Kitani A**. IL-13 signaling through the IL-13alpha2 receptor is involved in induction of TGF-beta1 production and fibrosis. *Nature medicine* 12: 99-106, 2006.
20. **Groom JR, Richmond J, Murooka TT, Sorensen EW, Sung JH, Bankert K, von Andrian UH, Moon JJ, Mempel TR, and Luster AD**. CXCR3 chemokine receptor-ligand interactions in the lymph node optimize CD4+ T helper 1 cell differentiation. *Immunity* 37: 1091-1103, 2012.
21. **Hancock A, Armstrong L, Gama R, and Millar A**. Production of interleukin 13 by alveolar macrophages from normal and fibrotic lung. *American journal of respiratory cell and molecular biology* 18: 60-65, 1998.
22. **Hasegawa M, Fujimoto M, Kikuchi K, and Takehara K**. Elevated serum levels of interleukin 4 (IL-4), IL-10, and IL-13 in patients with systemic sclerosis. *The Journal of rheumatology* 24: 328-332, 1997.
23. **Hayashi T, Stetler-Stevenson WG, Fleming MV, Fishback N, Koss MN, Liotta LA, Ferrans VJ, and Travis WD**. Immunohistochemical study of metalloproteinases and their tissue inhibitors in the lungs of patients with diffuse alveolar damage and idiopathic pulmonary fibrosis. *Am J Pathol* 149: 1241-1256, 1996.
24. **Hinz B, Celetta G, Tomasek JJ, Gabbiani G, and Chaponnier C**. Alpha-smooth muscle actin expression upregulates fibroblast contractile activity. *Molecular biology of the cell* 12: 2730-2741, 2001.
25. **Hinz B, Phan SH, Thannickal VJ, Prunotto M, Desmouliere A, Varga J, De Wever O, Mareel M, and Gabbiani G**. Recent developments in myofibroblast biology: paradigms for connective tissue remodeling. *Am J Pathol* 180: 1340-1355, 2012.

26. **Jakubzick C, Choi ES, Joshi BH, Keane MP, Kunkel SL, Puri RK, and Hogaboam CM**. Therapeutic attenuation of pulmonary fibrosis via targeting of IL-4- and IL-13-responsive cells. *Journal of immunology (Baltimore, Md : 1950)* 171: 2684-2693, 2003.
27. **Jiang D, Liang J, Campanella GS, Guo R, Yu S, Xie T, Liu N, Jung Y, Homer R, Meltzer EB, Li Y, Tager AM, Goetinck PF, Luster AD, and Noble PW**. Inhibition of pulmonary fibrosis in mice by CXCL10 requires glycosaminoglycan binding and syndecan-4. *The Journal of clinical investigation* 120: 2049-2057, 2010.
28. **Jiang D, Liang J, Hodge J, Lu B, Zhu Z, Yu S, Fan J, Gao Y, Yin Z, Homer R, Gerard C, and Noble PW**. Regulation of pulmonary fibrosis by chemokine receptor CXCR3. *The Journal of clinical investigation* 114: 291-299, 2004.
29. **Kato T, Saeki H, Tsunemi Y, Shibata S, Tamaki K, and Sato S**. Thymus and activation-regulated chemokine (TARC)/CC chemokine ligand (CCL) 17 accelerates wound healing by enhancing fibroblast migration. *Experimental dermatology* 20: 669-674, 2011.
30. **Keane MP, Belperio JA, Arenberg DA, Burdick MD, Xu ZJ, Xue YY, and Strieter RM**. IFN-gamma-inducible protein-10 attenuates bleomycin-induced pulmonary fibrosis via inhibition of angiogenesis. *Journal of immunology (Baltimore, Md : 1950)* 163: 5686-5692, 1999.
31. **Keane MP, Gomperts BN, Weigt S, Xue YY, Burdick MD, Nakamura H, Zisman DA, Ardehali A, Saggar R, Lynch JP, 3rd, Hogaboam C, Kunkel SL, Lukacs NW, Ross DJ, Grusby MJ, Strieter RM, and Belperio JA**. IL-13 is pivotal in the fibro-obliterative process of bronchiolitis obliterans syndrome. *Journal of immunology (Baltimore, Md : 1950)* 178: 511-519, 2007.
32. **Kolodsick JE, Toews GB, Jakubzick C, Hogaboam C, Moore TA, McKenzie A, Wilke CA, Chrisman CJ, and Moore BB**. Protection from fluorescein isothiocyanate-induced fibrosis in IL-13-deficient, but not IL-4-deficient, mice results from impaired collagen synthesis by fibroblasts. *Journal of immunology (Baltimore, Md : 1950)* 172: 4068-4076, 2004.
33. **Kotsimbos TC, Ernst P, and Hamid QA**. Interleukin-13 and interleukin-4 are coexpressed in atopic asthma. *Proceedings of the Association of American Physicians* 108: 368-373, 1996.
34. **Kouroumalis A, Nibbs RJ, Aptel H, Wright KL, Kolios G, and Ward SG**. The chemokines CXCL9, CXCL10, and CXCL11 differentially stimulate G alpha i-independent signaling and actin responses in human intestinal myofibroblasts. *Journal of immunology (Baltimore, Md : 1950)* 175: 5403-5411, 2005.
35. **Kroeze KL, Boink MA, Sampat-Sardjoepersad SC, Waaijman T, Scheper RJ, and Gibbs S**. Autocrine regulation of re-epithelialization after wounding by chemokine receptors CCR1, CCR10, CXCR1, CXCR2, and CXCR3. *The Journal of investigative dermatology* 132: 216-225, 2012.
36. **Laragione T, Brenner M, Sherry B, and Gulko PS**. CXCL10 and its receptor CXCR3 regulate synovial fibroblast invasion in rheumatoid arthritis. *Arthritis and rheumatism* 63: 3274-3283, 2011.
37. **Loetscher M, Loetscher P, Brass N, Meese E, and Moser B**. Lymphocyte-specific chemokine receptor CXCR3: regulation, chemokine binding and gene localization. *European journal of immunology* 28: 3696-3705, 1998.
38. **Lumsden RV, Worrell JC, Boylan D, Walsh SM, Cramton J, Counihan I, O'Beirne S, Medina MF, Gauldie J, Fabre A, Donnelly SC, Kane R, and Keane**

MP. Modulation of pulmonary fibrosis by IL-13Ralpha2. *American journal of physiology Lung cellular and molecular physiology* 308: L710-718, 2015.
39. **Lupardus PJ, Birnbaum ME, and Garcia KC**. Molecular basis for shared cytokine recognition revealed in the structure of an unusually high affinity complex between IL-13 and IL-13Ralpha2. *Structure* 18: 332-342, 2010.
40. **Masuoka M, Shiraishi H, Ohta S, Suzuki S, Arima K, Aoki S, Toda S, Inagaki N, Kurihara Y, Hayashida S, Takeuchi S, Koike K, Ono J, Noshiro H, Furue M, Conway SJ, Narisawa Y, and Izuhara K**. Periostin promotes chronic allergic inflammation in response to Th2 cytokines. *The Journal of clinical investigation* 122: 2590-2600, 2012.
41. **Meiser A, Mueller A, Wise EL, McDonagh EM, Petit SJ, Saran N, Clark PC, Williams TJ, and Pease JE**. The chemokine receptor CXCR3 is degraded following internalization and is replenished at the cell surface by de novo synthesis of receptor. *Journal of immunology (Baltimore, Md : 1950)* 180: 6713-6724, 2008.
42. **Meyer M, Hensbergen PJ, van der Raaij-Helmer EM, Brandacher G, Margreiter R, Heufler C, Koch F, Narumi S, Werner ER, Colvin R, Luster AD, Tensen CP, and Werner-Felmayer G**. Cross reactivity of three T cell attracting murine chemokines stimulating the CXC chemokine receptor CXCR3 and their induction in cultured cells and during allograft rejection. *European journal of immunology* 31: 2521-2527, 2001.
43. **Murray LA, Argentieri RL, Farrell FX, Bracht M, Sheng H, Whitaker B, Beck H, Tsui P, Cochlin K, Evanoff HL, Hogaboam CM, and Das AM**. Hyper-responsiveness of IPF/UIP fibroblasts: interplay between TGFbeta1, IL-13 and CCL2. *The international journal of biochemistry & cell biology* 40: 2174-2182, 2008.
44. **O'Beirne SL, Walsh SM, Fabre A, Reviriego C, Worrell JC, Counihan IP, Lumsden RV, Cramton-Barnes J, Belperio JA, Donnelly SC, Boylan D, Marchal-Somme J, Kane R, and Keane MP**. CXCL9 Regulates TGF-beta1-Induced Epithelial to Mesenchymal Transition in Human Alveolar Epithelial Cells. *Journal of immunology (Baltimore, Md : 1950)* 195: 2788-2796, 2015.
45. **O'Reilly S, Ciechomska M, Fullard N, Przyborski S, and van Laar JM**. IL-13 mediates collagen deposition via STAT6 and microRNA-135b: a role for epigenetics. *Scientific reports* 6: 25066, 2016.
46. **Oghumu S, Varikuti S, Terrazas C, Kotov D, Nasser MW, Powell CA, Ganju RK, and Satoskar AR**. CXCR3 deficiency enhances tumor progression by promoting macrophage M2 polarization in a murine breast cancer model. *Immunology* 143: 109-119, 2014.
47. **Park SW, Ahn MH, Jang HK, Jang AS, Kim DJ, Koh ES, Park JS, Uh ST, Kim YH, Park JS, Paik SH, Shin HK, Youm W, and Park CS**. Interleukin-13 and its receptors in idiopathic interstitial pneumonia: clinical implications for lung function. *Journal of Korean medical science* 24: 614-620, 2009.
48. **Petrai I, Rombouts K, Lasagni L, Annunziato F, Cosmi L, Romanelli RG, Sagrinati C, Mazzinghi B, Pinzani M, Romagnani S, Romagnani P, and Marra F**. Activation of p38(MAPK) mediates the angiostatic effect of the chemokine receptor CXCR3-B. *The international journal of biochemistry & cell biology* 40: 1764-1774, 2008.
49. **Quelle FW, Shimoda K, Thierfelder W, Fischer C, Kim A, Ruben SM, Cleveland JL, Pierce JH, Keegan AD, Nelms K, and et al.** Cloning of murine Stat6 and human Stat6, Stat proteins that are tyrosine phosphorylated in responses to IL-4 and IL-3 but are not required for mitogenesis. *Molecular and cellular biology* 15: 3336-3343, 1995.

50. **Romagnani P, Annunziato F, Lasagni L, Lazzeri E, Beltrame C, Francalanci M, Uguccioni M, Galli G, Cosmi L, Maurenzig L, Baggiolini M, Maggi E, Romagnani S, and Serio M**. Cell cycle-dependent expression of CXC chemokine receptor 3 by endothelial cells mediates angiostatic activity. *The Journal of clinical investigation* 107: 53-63, 2001.
51. **Sauty A, Colvin RA, Wagner L, Rochat S, Spertini F, and Luster AD**. CXCR3 internalization following T cell-endothelial cell contact: preferential role of IFN-inducible T cell alpha chemoattractant (CXCL11). *Journal of immunology (Baltimore, Md : 1950)* 167: 7084-7093, 2001.
52. **Shelfoon C, Shariff S, Traves SL, Kooi C, Leigh R, and Proud D**. Chemokine release from human rhinovirus-infected airway epithelial cells promotes fibroblast migration. *The Journal of allergy and clinical immunology* 138: 114-122.e114, 2016.
53. **Smith RS, Smith TJ, Blieden TM, and Phipps RP**. Fibroblasts as sentinel cells. Synthesis of chemokines and regulation of inflammation. *The American journal of pathology* 151: 317-322, 1997.
54. **Swaisgood CM, French EL, Noga C, Simon RH, and Ploplis VA**. The development of bleomycin-induced pulmonary fibrosis in mice deficient for components of the fibrinolytic system. *Am J Pathol* 157: 177-187, 2000.
55. **Tighe RM, Liang J, Liu N, Jung Y, Jiang D, Gunn MD, and Noble PW**. Recruited exudative macrophages selectively produce CXCL10 after noninfectious lung injury. *American journal of respiratory cell and molecular biology* 45: 781-788, 2011.
56. **Walsh SM, Worrell JC, Fabre A, Hinz B, Kane R, and Keane MP**. Novel differences in gene expression and functional capabilities of myofibroblast populations in idiopathic pulmonary fibrosis. *American journal of physiology Lung cellular and molecular physiology* 315: L697-l710, 2018.
57. **Werner S, and Grose R**. Regulation of wound healing by growth factors and cytokines. *Physiological reviews* 83: 835-870, 2003.
58. **Wohlfahrt T, Rauber S, Uebe S, Luber M, Soare A, Ekici A, Weber S, Matei A-E, Chen C-W, Maier C, Karouzakis E, Kiener HP, Pachera E, Dees C, Beyer C, Daniel C, Gelse K, Kremer AE, Naschberger E, Stürzl M, Butter F, Sticherling M, Finotto S, Kreuter A, Kaplan MH, Jüngel A, Gay S, Nutt SL, Boykin DW, Poon GMK, Distler O, Schett G, Distler JHW, and Ramming A**. PU.1 controls fibroblast polarization and tissue fibrosis. *Nature* 566: 344-349, 2019.
59. **Wood N, Whitters MJ, Jacobson BA, Witek J, Sypek JP, Kasaian M, Eppihimer MJ, Unger M, Tanaka T, Goldman SJ, Collins M, Donaldson DD, and Grusby MJ**. Enhanced interleukin (IL)-13 responses in mice lacking IL-13 receptor alpha 2. *The Journal of experimental medicine* 197: 703-709, 2003.
60. **Wynn TA, and Barron L**. Macrophages: master regulators of inflammation and fibrosis. *Seminars in liver disease* 30: 245-257, 2010.
61. **Yates CC, Krishna P, Whaley D, Bodnar R, Turner T, and Wells A**. Lack of CXC chemokine receptor 3 signaling leads to hypertrophic and hypercellular scarring. *Am J Pathol* 176: 1743-1755, 2010.
62. **Yates CC, Whaley D, Kulasekeran P, Hancock WW, Lu B, Bodnar R, Newsome J, Hebda PA, and Wells A**. Delayed and deficient dermal maturation in mice lacking the CXCR3 ELR-negative CXC chemokine receptor. *Am J Pathol* 171: 484-495, 2007.

63. **Yates CC, Whaley D, and Wells A**. Transplanted fibroblasts prevents dysfunctional repair in a murine CXCR3-deficient scarring model. *Cell Transplant* 21: 919-931, 2012.
64. **Zhu Z, Homer RJ, Wang Z, Chen Q, Geba GP, Wang J, Zhang Y, and Elias JA**. Pulmonary expression of interleukin-13 causes inflammation, mucus hypersecretion, subepithelial fibrosis, physiologic abnormalities, and eotaxin production. *The Journal of clinical investigation* 103: 779-788, 1999.
65. **Zurawski SM, Chomarat P, Djossou O, Bidaud C, McKenzie AN, Miossec P, Banchereau J, and Zurawski G**. The primary binding subunit of the human interleukin-4 receptor is also a component of the interleukin-13 receptor. *The Journal of biological chemistry* 270: 13869-13878, 1995.

Figure Legends

Figure 1

Regulation of CXCR3 and IL-13Rα2 by CXCR3 ligands. qRT-PCR was used to quantify mRNA expression of *Cxcr3A* (A) and *Il13rα2* (B) in NIH3T3 fibroblasts treated with CXCR3 ligands CXCL9 (10ng/ml), CXCL10 (10ng/ml) or vehicle control for 24 h. (C) sIL-13Rα2 (pg/ml) detected by ELISA (D) Cellular proliferation was measured using a BrdU assay (n=5). (E) mRNA expression of *Il13rα2* in NIH3T3 fibroblasts treated with CXCR3 antagonist 1 hour prior to stimulation with CXCL9, CXCL10 or vehicle for 24 h. (G) Cell viability was measured by Alamar blue assay and (H) proliferation by BrdU assay following treatment with CXCR3 antagonist or vehicle control at 24 h. Data analysed using the ΔΔCt method and presented as fold change versus vehicle control. Two-tailed Student's *t*-test for pairwise comparison of variables, one-way ANOVA for multiple comparison of variables, a Sidak's multiple comparisons test was used. Data presented as mean ± SEM and representative of (n=3) independent experiments unless otherwise stated. Student's t-test for *$p< 0.05$, ** $p < 0.01$.

Figure 2

Immunofluorescent staining of NIH3T3 fibroblasts seeded on glass chamber slides transfected with either empty vector control or CXCR3A plasmid for 24 h. (A) Fibroblasts were stained with anti-CXCR3-PE labelled Ab (yellow) or isotype control antibody. Nuclei were counterstained with DAPI (blue). Images were digitally captured using Axiovision software version 4.8 (original magnification x400). Experiments were repeated independently three times, and representative images are

shown (scale bars 20μm). (B) Cell viability was measured by Alamar blue assay (n=3). (C)qRT-PCR was used to determine *Cxcr3A* mRNA expression using the ΔΔCt method of analysis (n=5). Data presented as fold change compared to empty vector control. Data represented as mean ± SEM. Two-tailed Student's *t*-test,**P <0.01 (D) WCEs (whole cell extracts) were obtained from empty vector controls or CXCR3A transfected fibroblasts, Western blotting was performed CXCR3A with β-actin as a loading control. Data representative of (n=3) independent experiments.

Figure 3

Fibrogenic gene expression, cellular proliferation and production of soluble mediators following CXCR3A overexpression. NIH3T3 fibroblasts were transfected with either empty vector control or CXCR3A plasmid for 24 h. mRNA expression levels of fibrogenic genes (A) *Acta2*, (B) *Col1a1*, (C) *Vim,* (D) *Fsp1* and the anti-fibrotic receptor (E) *Il13ra2* were quantified using the ΔΔCt method of analysis. Data presented as fold change compared to empty vector controls. Data representative of (n=5) independent experiments. Functional assays measured proliferation (F) BrdU assay and soluble collagen production (G) Sircol assay (μg/ml). Release of soluble mediators in cell supernatants (H) active-TGFβ1 production (pg/ml), (I) CXCL9 (pg/ml) and (J) CXCL10 (pg/ml) was quantified by ELISA. All data are presented as mean ± SEM and are representative of (n=4) independent experiments unless otherwise stated. Two-tailed Student's *t*-test, * P < 0.05, ***P <0.001.

Figure 4

Downstream signalling and release of soluble mediators in NIH3T3 fibroblasts transfected with either empty vector control or CXCR3A plasmid for 24 h in response to IL-13 stimulation. (A) WCEs were obtained from empty vector controls or

CXCR3A transfected fibroblasts stimulated with IL-13 (10ng/ml) for 0-120 mins. (A) Western blotting was performed for phosphorylated and total forms of STAT6, ERK1/2 and NFκB-p65 with β-actin as a loading control. (B) Western blotting was performed for IL-13Rα2 following transfection for 24 and stimulation with IL-13 (10ng/ml) for a further 24 h. Data are representative of (n=3) independent experiments, representative images are shown. Release of soluble mediators in cell supernatants was quantified by ELISA (C) soluble IL-13Rα2 (sIL-13Rα2, pg/ml) and (D) Periostin (pg/ml). All data are presented as mean ± SEM and are representative of (n=3) independent experiments unless otherwise stated. One-way ANOVA for multiple comparison of variables, a Sidak's multiple comparisons test was used, *P<0.05.

Figure 5

CXCR3A$^{-/-}$ fibroblasts have reduced contractility, increased proliferative capacity and soluble collagen production. WT and CXCR3A$^{-/-}$ fibroblasts treated with IL-13 (10ng/ml) for 24h on fibronectin-coated elastic wrinkling silicone substrates. (A) Top panel are phase contrast images showing contracting cells that produced wrinkles in the soft silicone substrate surface after treatment with IL-13 (10 ng/ml) for 24 h. (B) Bottom panel are thresholded for phase-bright wrinkles and binarized in ImageJ. (C) Coverage of wrinkles from binarized images was calculated as percentage area covered. Values are presented as mean ± SEM . At least 4 regions were analyzed per experimental condition. Scale bars represent 50μm. (D) Basal soluble collagen production (μg/mL) and (E) cellular proliferation measured by BrdU assay. (F) WCEs were obtained from WT and CXCR3A$^{-/-}$ fibroblasts cultured under basal conditions,

Western blotting was performed for fibroblast activation and contractility markers Col1A1, Vimentin and α-SMA with β-actin as a loading control. All experiments were performed independently 3 times, representative images are shown.

Figure 6

IL-13 regulates chemokine expression and alveolar macrophage accumulation *in vivo*. BAL fluid was aspirated from the lungs of mice 24 h post intranasal administration of 10μg/ml IL-13 or vehicle (PBS). A total cell count per sample was measured (10^4 cells /ml). (B) CXCL10 (pg/ml) levels in cell free BAL were quantified by ELISA (C) Diffquik staining ($1x10^4$) cells per sample was used to stain cells present in the lavage fluid, black arrows indicate alveolar macrophages, scale bars representative of 100μm and 25μm on enlarged images. (n=5) animals per group for BAL analysis with the exception of WT vehicle (n=3). Protein levels were quantified in lung homogenates (D) CXCL9 (pg/ml), (E) CXCL10 (pg/ml) and soluble IL-13Rα2 (pg/ml) (n=6 mice per group). Data are presented as mean ± SEM and analysed using a two-way ANOVA involving two independent variables. A Sidak's multiple comparisons test was used. *$p< 0.05$, ** $p < 0.01$, *** $p <0.001$.

Figure 7

Cxcr3A is downregulated by IL-13 *in vitro* and *in vivo* in response to chronic lung fibrosis. (A) Cxcr3A mRNA expression. Data analysed using the ΔΔCt method and presented as fold change versus vehicle control. Data presented as mean ± SEM and representative of (n=6) independent experiments. (B) WCEs (whole cell extracts) were obtained from NIH3T3 fibroblasts treated with IL-13 (10ng/ml) or vehicle for 24 h. Western blotting was performed for CXCR3A with β-actin as a loading control. (C) sIL-13Rα2 (pg/ml) in NIH3T3 fibroblasts treated with IL-13 (10ng/ml) or vehicle for

24 h. Two-tailed Student's t test for pairwise comparison of variables * P <0.05, ** P < 0.01. (D) Cxcr3A mRNA expression in WT murine lungs following bleomycin instillation at day 5 (inflammatory phase, n=14) or day 21 (fibrotic phase, n=11) versus sham controls (n=15). Data analysed using the ΔΔCt method and presented as fold change versus vehicle control. One-way ANOVA for multiple comparison of variables, a Sidak's multiple comparisons test was used, *** P < 0.001.

Figure 1

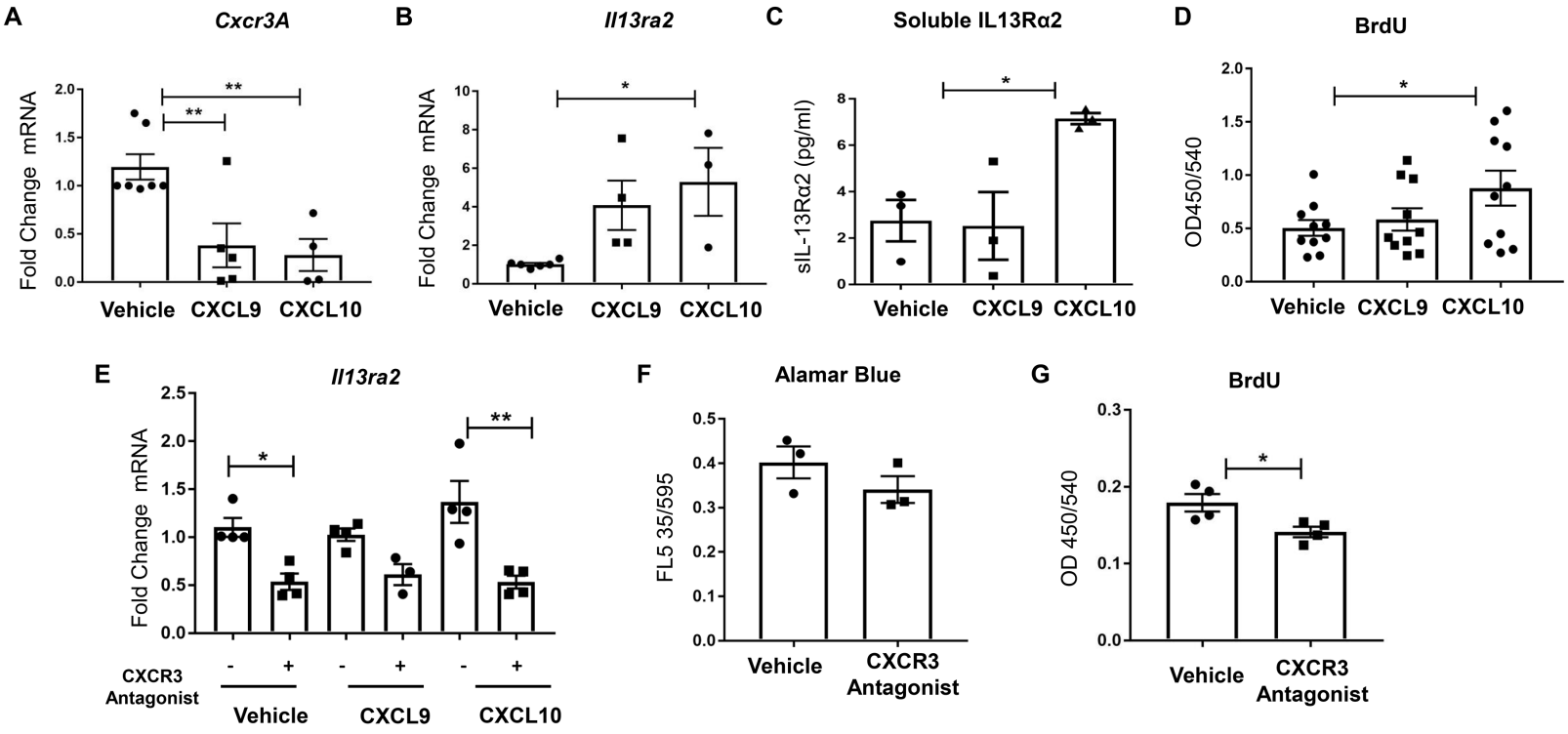
A
Cxcr3A
Fold Change mRNA
Vehicle
CXCL9
CXCL10
B
Il13ra2
Fold Change mRNA
C
Soluble IL13Rα2
sIL-13Rα2 (pg/ml)
D
BrdU
OD450/540
E
Il13ra2
Fold Change mRNA
CXCR3 Antagonist
F
Alamar Blue
FL5 35/595
G
BrdU
OD 450/540
CXCR3 Antagonist

Figure 2

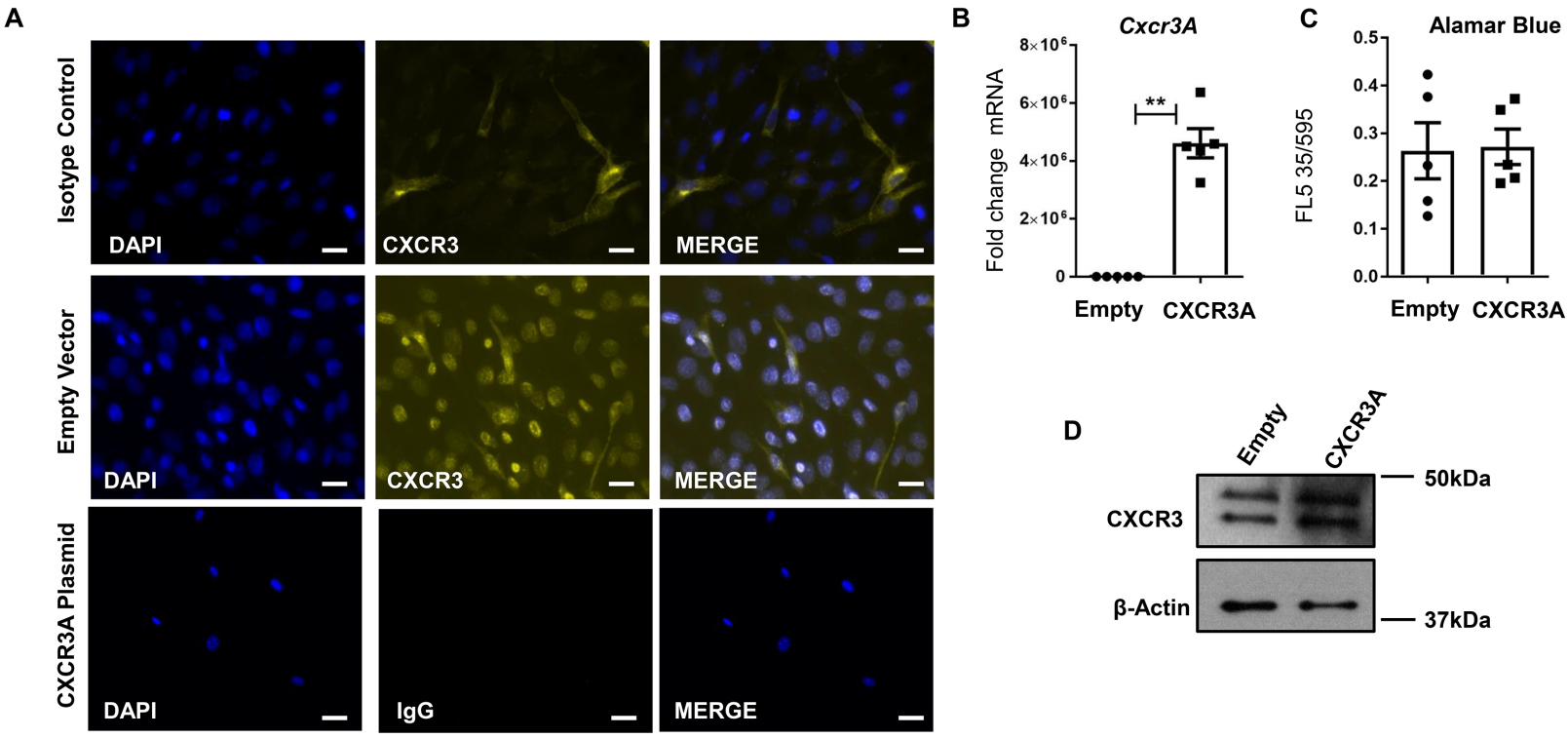
A
Isotype Control
Empty Vector
CXCR3A Plasmid
DAPI
CXCR3
MERGE
IgG
B
Cxcr3A
Fold change mRNA
8×10⁶
6×10⁶
4×10⁶
2×10⁶
0
**
Empty
CXCR3A
C
Alamar Blue
FL5 35/595
0.5
0.4
0.3
0.2
0.1
0.0
Empty
CXCR3A
D
Empty
CXCR3A
CXCR3
β-Actin
50kDa
37kDa

Figure 3

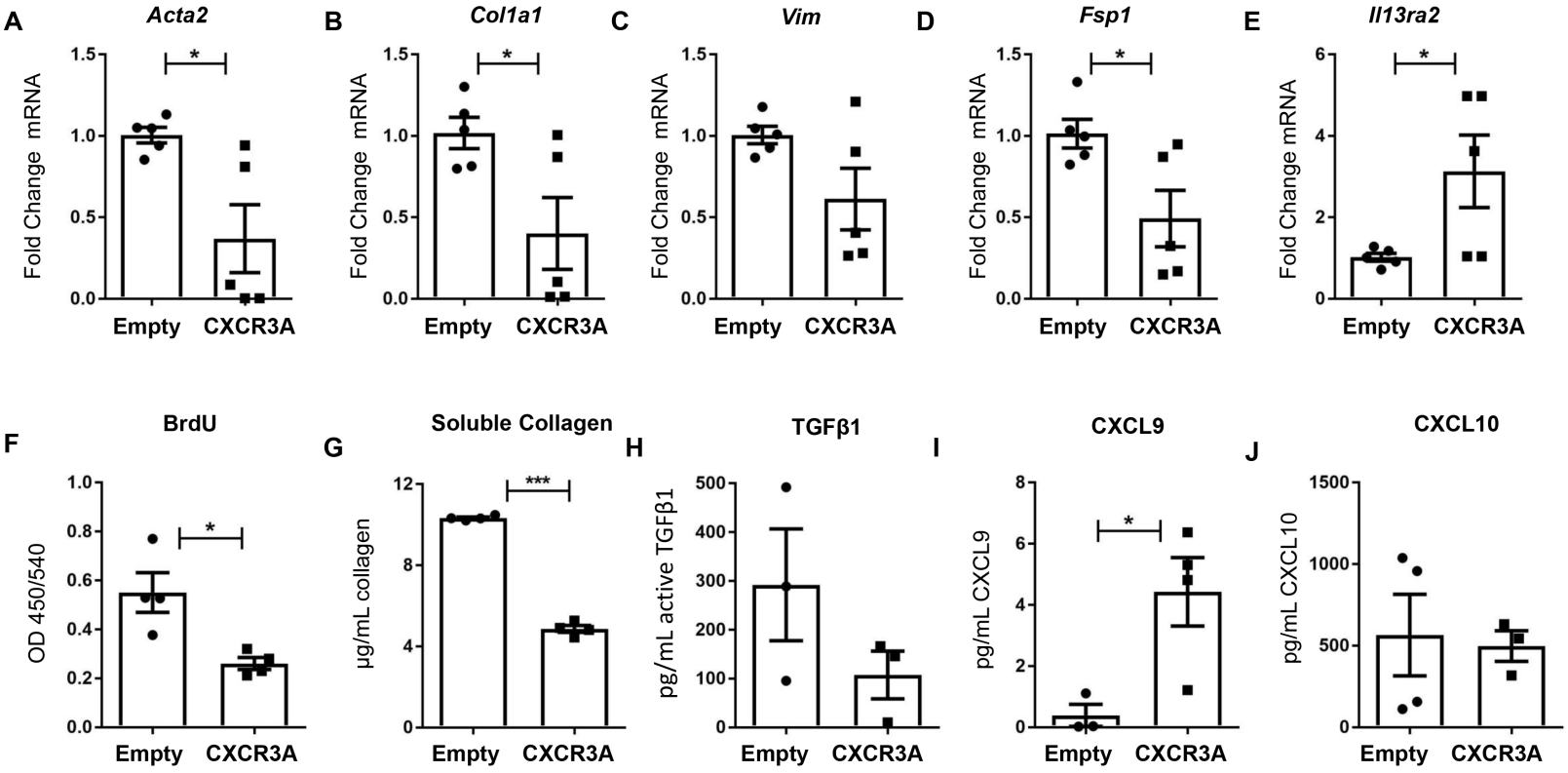
A
Acta2
Fold Change mRNA
1.5
1.0
0.5
0.0
*
Empty
CXCR3A
B
Col1a1
Fold Change mRNA
1.5
1.0
0.5
0.0
*
Empty
CXCR3A
C
Vim
Fold Change mRNA
1.5
1.0
0.5
0.0
Empty
CXCR3A
D
Fsp1
Fold Change mRNA
1.5
1.0
0.5
0.0
*
Empty
CXCR3A
E
Il13ra2
Fold Change mRNA
6
4
2
0
*
Empty
CXCR3A
F
BrdU
OD 450/540
1.0
0.8
0.6
0.4
0.2
0.0
*
Empty
CXCR3A
G
Soluble Collagen
µg/mL collagen
12
8
4
0
***
Empty
CXCR3A
H
TGFβ1
pg/mL active TGFβ1
500
400
300
200
100
0
Empty
CXCR3A
I
CXCL9
pg/mL CXCL9
8
6
4
2
0
*
Empty
CXCR3A
J
CXCL10
pg/mL CXCL10
1500
1000
500
0
Empty
CXCR3A

Figure 4

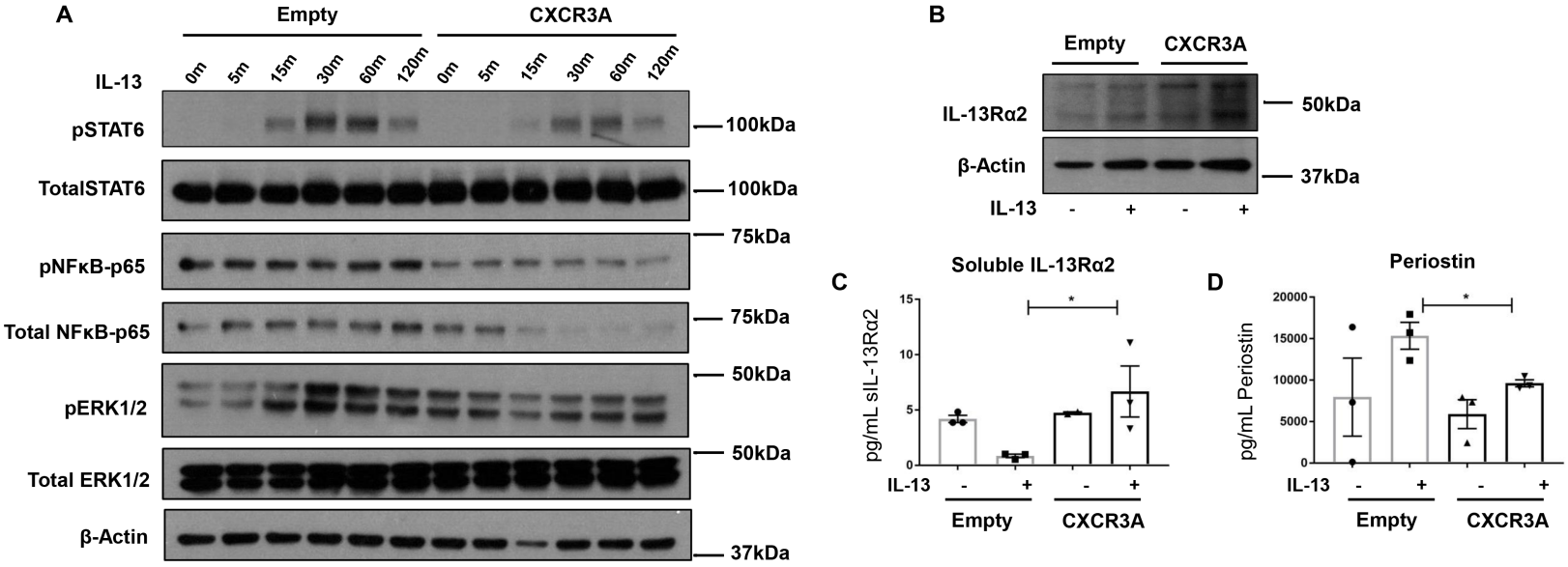
A
Empty
CXCR3A
IL-13
0m
5m
15m
30m
60m
120m
pSTAT6
TotalSTAT6
pNFκB-p65
Total NFκB-p65
pERK1/2
Total ERK1/2
β-Actin
100kDa
100kDa
75kDa
75kDa
50kDa
50kDa
37kDa
B
Empty
CXCR3A
IL-13Rα2
β-Actin
50kDa
37kDa
IL-13
C
Soluble IL-13Rα2
pg/mL sIL-13Rα2
IL-13
Empty
CXCR3A
D
Periostin
pg/mL Periostin
IL-13
Empty
CXCR3A

Figure 5

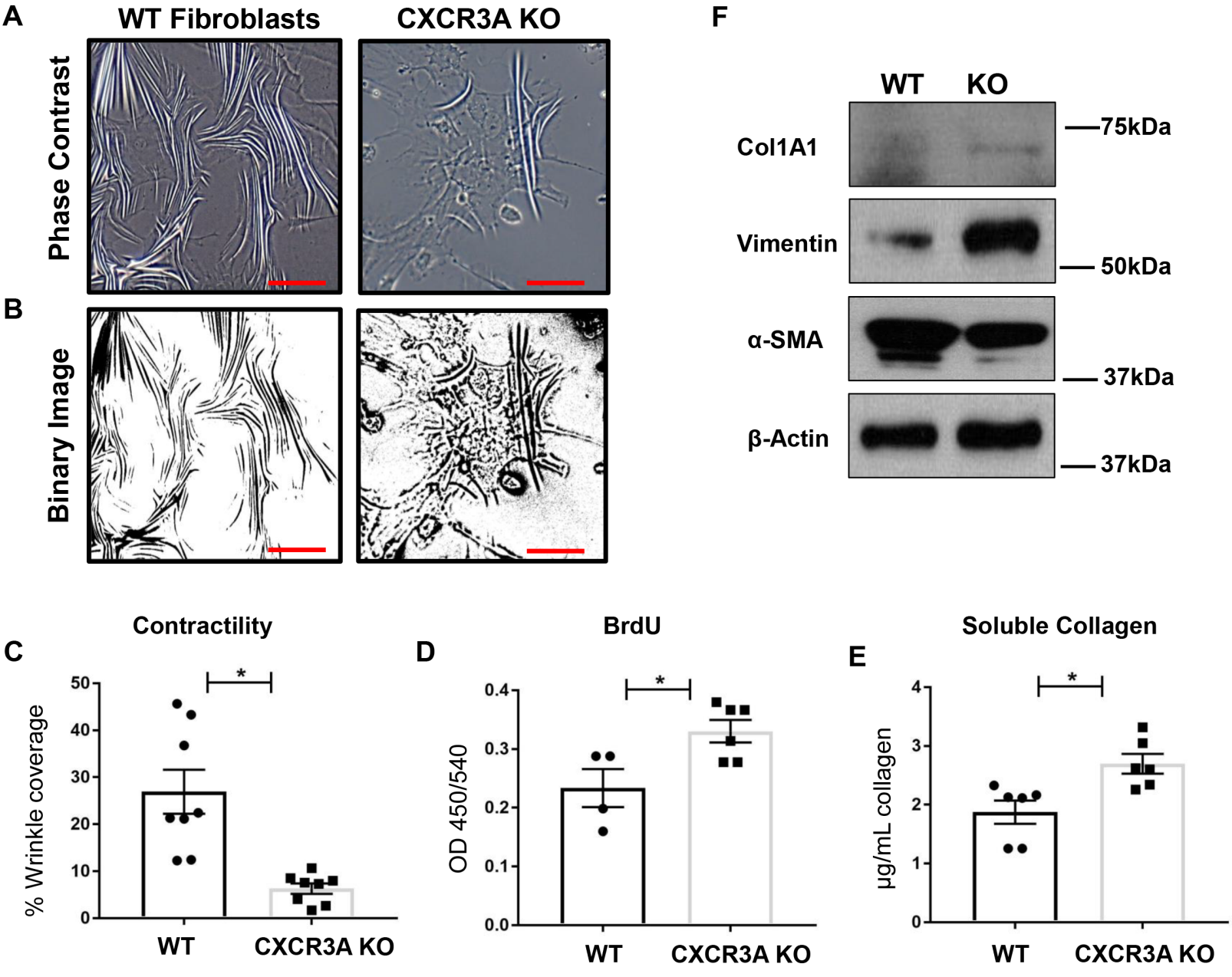
A
WT Fibroblasts
CXCR3A KO
Phase Contrast
B
Binary Image
F
WT
KO
Col1A1
75kDa
Vimentin
50kDa
α-SMA
37kDa
β-Actin
37kDa
Contractility
C
% Wrinkle coverage
50
40
30
20
10
0
*
WT
CXCR3A KO
BrdU
D
OD 450/540
0.4
0.3
0.2
0.1
0.0
*
WT
CXCR3A KO
Soluble Collagen
E
µg/mL collagen
4
3
2
1
0
*
WT
CXCR3A KO

Figure 6

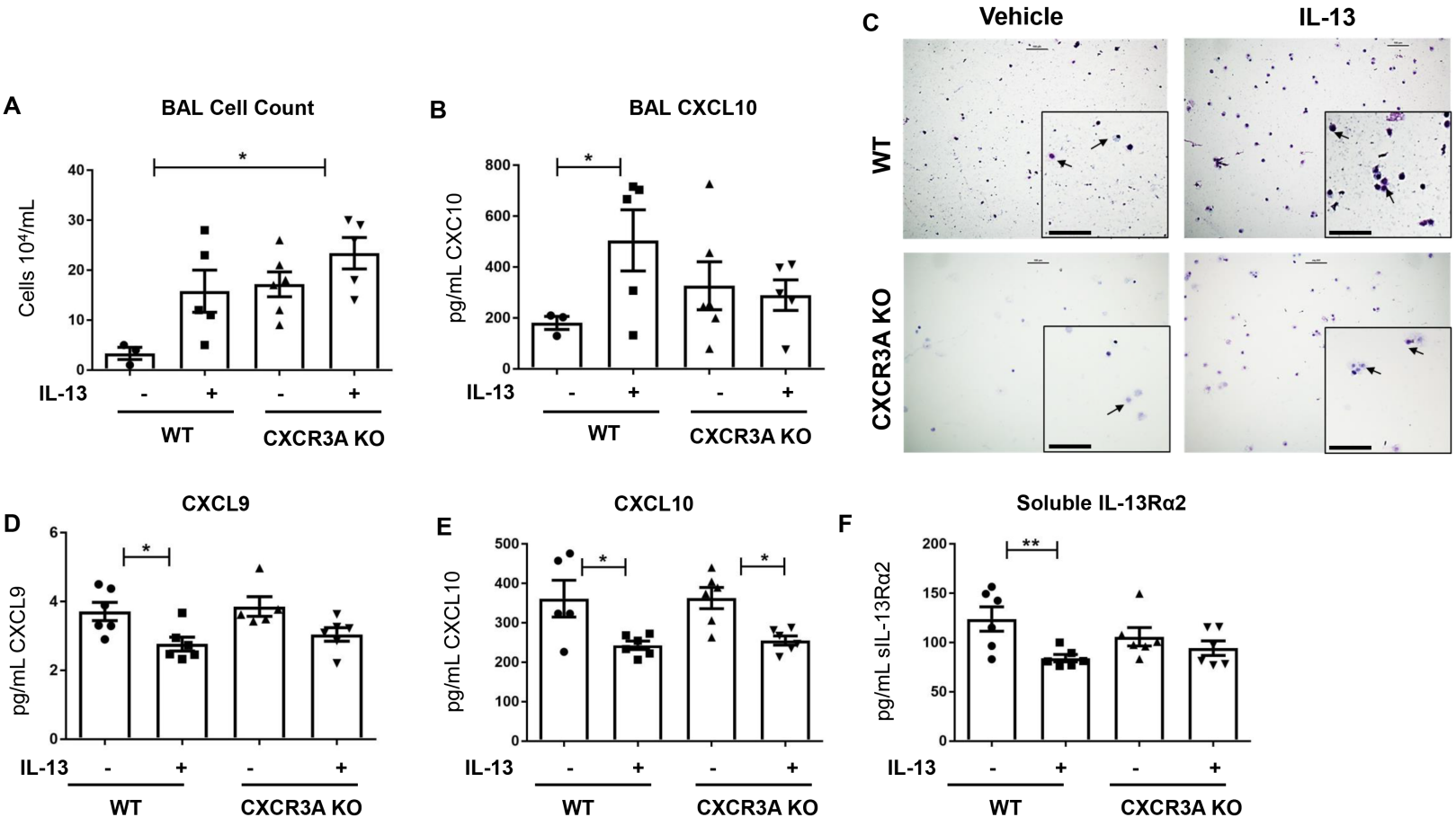
A
BAL Cell Count
Cells 10⁴/mL
IL-13
WT
CXCR3A KO
B
BAL CXCL10
pg/mL CXC10
C
Vehicle
IL-13
WT
CXCR3A KO
D
CXCL9
pg/mL CXCL9
E
CXCL10
pg/mL CXCL10
F
Soluble IL-13Rα2
pg/mL sIL-13Rα2

Figure 7

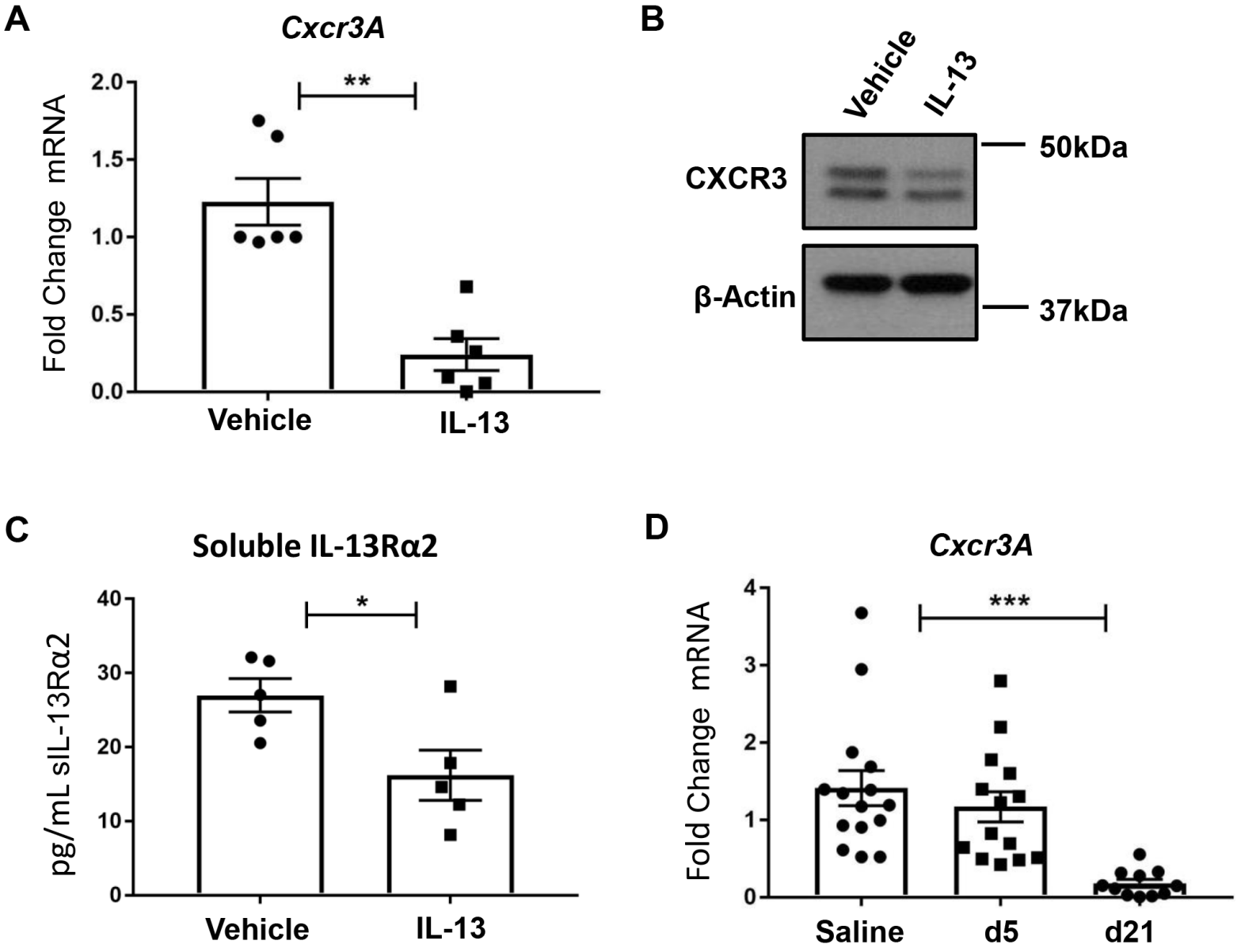
A
Cxcr3A
Fold Change mRNA
2.0
1.5
1.0
0.5
0.0
**
Vehicle
IL-13
B
Vehicle
IL-13
CXCR3
50kDa
β-Actin
37kDa
C
Soluble IL-13Rα2
pg/mL sIL-13Rα2
40
30
20
10
0
*
Vehicle
IL-13
D
Cxcr3A
Fold Change mRNA
4
3
2
1
0
***
Saline
d5
d21